

Shape Control of Variable Guide Frame for Tunnel Wall Inspection

F. Inoue^a, S. Kwon^a, T. Uchiyama^a, S. Nakamura^b and Y. Yanagihara^b

^aShonan Institute of Technology, Japan, ^bTokyu Construction, Japna
E-mail: Inoue@mech.shonan-it.ac.jp

Abstract

To progress the automated inspection and maintenance of inner wall of tunnel, the advanced inspection system with restricting the traffic regulation was developed. In this inspection system, the guide frame along tunnel wall was installed on the protection unit stepped over the road like gantry crane. The inspection device moved with stability by adopting the guide frame, and the inspection accuracy could be improved. However, when this unit moved along the tunnel, this guide frame should avoid the convex obstacles such as duct fan, lamp and several road traffic sign in the tunnel. Therefore, by composing the entire frame of VGT (Variable geometry Truss), the shape of guide frame was changed flexibly and it could be passed in the tunnel. As a shape control of the guide frame, the inverse analysis method was applied such as robot manipulator combining two fixed-length members in series. The angle of each frame was reversely analysed according to the shape of the obstacle measured with the laser sensor, and the actuator of the frame was controlled simultaneously. Applying such control method, the shape was transported smoothly to keep a steady structure of guide frame.

In this paper, the outline of tunnel wall inspection applied variable guide frame, the structure principle of the guide frame, basic method of shape analysis and control technology, the finding of convex obstacles by laser sensor and the whole inspection system are explained in detail.

Keywords –

Structure, Automated Inspection system, Shape Control, Tunnel Inspection, Variable Guide Frame Introduction

1 Introduction

Most of infrastructures for civil engineering structures such as highway roads, bridges, tunnels constructed around the urban region in high-growth era of 1970-1990 begun to reach the life, and it has been the time when large-scale repair and renewal, rebuilding were demanded. Since these structures are difficult to

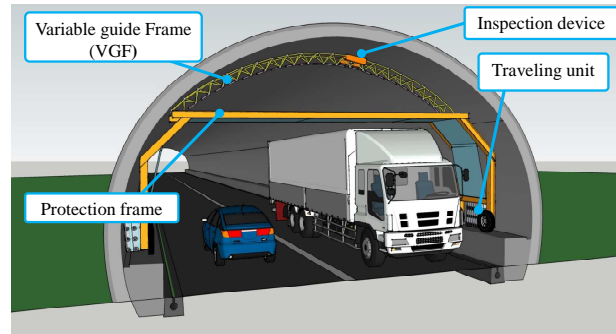


Fig. 1 Variable Guide Frame Vehicle for Inspection of Tunnel

renovate after completion, it is necessary to grasp the progress of deterioration by periodic inspection and to maintain and manage such as repair and renewal based on future prediction. Especially, with the collapse accident of the highway tunnel generated some time ago in Japan, the inspection of the superannuated tunnel was requested.

Generally, in the periodic inspection of the road tunnel, a maintenance engineer approached the wall by using mobile elevating work platform as much as possible and by restricting the traffic regulation and the engineers detected the deteriorated wall parts by sighting and hammering sound. To progress the automated inspection and maintenance of inner wall of tunnel, some advanced methods were adopted in the SIP program in Japan of the theme of "Maintenance and management robot". In our proposal of this theme, the inspection system was developed applying the variable guide frame to evade the obstacle in the tunnel without restriction of the traffic regulation as indicating in Fig. 1. In this inspection system, this guide frame was installed on the protection frame with travelling unit. When this unit moved along the tunnel, the guide frame should avoid the obstacles such as traffic plate, lamp and discharged ducts in the tunnel. The shape of this guide frame changing flexibly, the frame was able to pass these obstacles in the tunnel easily [1], [2].

In this paper, a method of searching for obstacles in a tunnel using three dimension laser range finder of the high-resolution evaluation, a method of controlling a frame whose shape can be changed according to the obstacles shape, and its experiment results are described.

2 Obstacles Detection in Tunnel

Since the positions and shapes of the various obstacles existing in the tunnel are described on the construction drawing of the tunnel, it is possible to change the shape of the frame so as to avoid obstacles. However, the guide frame being on the based truck, it is necessary to accurately measure the relative distance between the based truck and the obstacle. Also, because the movement error of the based truck is actually included, the obstacle search was carried out on the based truck at the site. In this chapter, Stereo measurement system, analysis method of the shape and position of the obstacle, and its measurement results were verified.

2.1 Stereo Measurement System Using Laser Rang Finder

As the base truck on which the guide frame is installed moves along the inner wall of the tunnel, obstacles protruding from the inner wall near the ceiling may come into contact with the guide frame. Here, as shown in Fig.2, the laser range finder (LRF) was installed at the center of the truck beam surface part and an obstacle on the ceiling surface of the tunnel roughly 1 to 5 m in front was searched. In order to explore the three dimensional space, as shown in Fig. 3, we connected the LRF to the pan unit and constructed the stereo measurement system giving its inclination angle θ_2 to the plane measurement area angle θ_1 of LRF. In this case, if the distance to an object measured by the reflection time of the laser is l , its coordinates (x, y, z) can be expressed by equation (1) - (3).

$$x = l \cdot \cos \theta_2 \cdot \cos \theta_1 \quad (1)$$

$$y = l \cdot \cos \theta_2 \cdot \sin \theta_1 \quad (2)$$

$$z = l \cdot \sin \theta_2 \quad (3)$$

The specification of LRF is indicated in Table 1. The range of measurement is 30[m], the scan time rate is 25[ms] and the resolution angle of rotating laser is 0.25 [deg]. The angular resolution of pan unit was 1.0 deg. at $\theta_2 \leq 10$ deg. and was 0.5 deg at $\theta_2 > 10$ deg, the measurement precision was increased as it approached the tunnel inner wall. In an actual measurement, the laser irradiated from LRF is reflected to the outer side of the object, and the distances on each object surface were measured from the principle of TOF (Time of flight).

As shown in Fig. 4, to ascertain the cross-sectional shape of the obstacle ahead from the based truck, the laser reflection points existing at the interval of Δy (= about 100 mm) with respect to the distance y from the based truck are counted. Then, it estimated that there is an obstacle in a certain y portion where the reflection points are strongly concentrated.

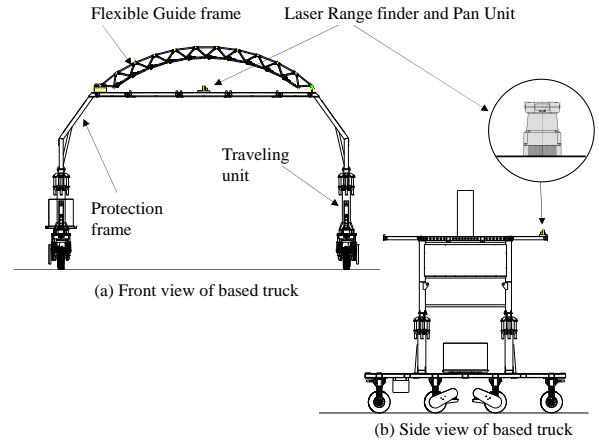


Fig.2 Structure of based truck and install of LRF on the truck

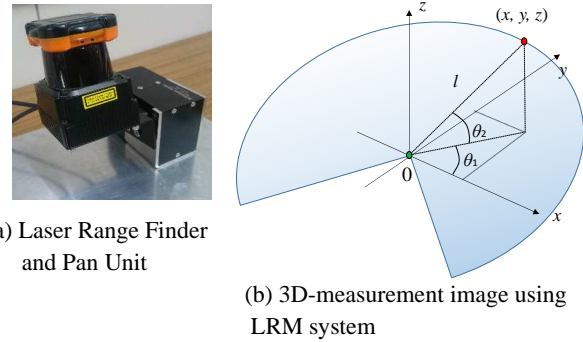


Fig. 3 Obstacle detection by stereo measurement system

Table 1 Specification of LRF

Model Number	UTM-30LX
Light Source	Laser Diode, $\lambda = 870$ nm
Measureable Area	0.1 ~ 30 m, 270 deg
Accuracy	0.1 ~ 10 m, ± 30 mm
	10 ~ 30 m, ± 50 mm
Angular Resolution	0.25 deg
Scan time	25 ms

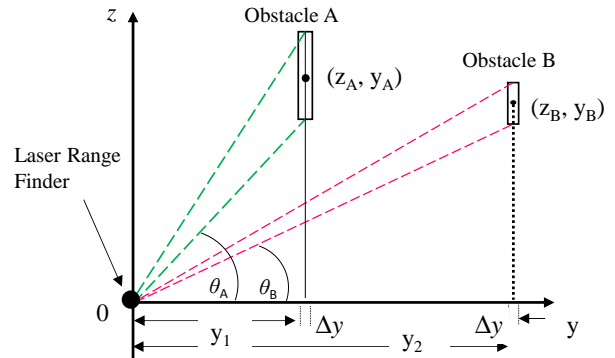


Fig. 4 Objects analysis in x-z coordinate by LRF in x-z coordinate

2.2 Position Analysis Method of Obstacles

In order to determine the cross-sectional position of the obstacle, the center position of the obstacle was analyzed assuming that the shape of the obstacle is a circle from the contour of the point group. By assuming that the obstacle is circular even if it is rectangular, the contour of the obstacle was estimated on the safe side.

Fig. 5 shows the analysis flow for estimating the position and shape of the obstacle.

①: First of all, scanned the inside of the tunnel with LRF and derived and recorded the laser reflection point. However, since the laser reflection points from the inner wall of the tunnel were geometrically known, their reflection points were deleted. As a result, the shape of the obstacle ahead of the truck was extracted.

②: We classified the start position and the end position where the laser reflection point of the obstacle is recorded and extracted the edge of the obstacle.

③: The center position of the circle was estimated using the Constant Distance Method (CDM) [3] and the Least Squares Method (LSM) [4], assuming that the point group constituting the edge is an arc of a circle. The CDM is defined a position advanced by a constant d from the cluster's center as a center position of the object (x_{obj}, y_{obj}) as shown in Fig.6 and described in by equation (4), (5).

$$x_{obj} = x_{cl} + d \cos \beta \quad (4)$$

$$y_{obj} = y_{cl} + d \sin \beta \quad (5)$$

The LSM for a circle is a method for estimating parameters a , b , and r which will minimize the square sum of the error J_{LS} expressed as

$$J_{LS} = \sum_{\alpha=1}^N [(x_{\alpha} - a)^2 + (y_{\alpha} - b)^2 - r^2]^2 \quad (6)$$

where (x_{α}, y_{α}) , $\alpha = 1, \dots, N$ are the observed data points belonging to the contour of the reference bar.

④: Finally, we confirmed the range that the shape change of the guide frame avoids with an extra margin against obstacles.

By repeating the above process, the shape and forward position of the obstacle to be avoided by the guide frame are determined [5].

2.3 Measurement Result of Obstacle

Using the real simulated tunnel constructed for the experiment as indicated in Fig.7, the obstacles attached to the inner wall of tunnel was measured by LMS. Fig. 8 shows the state of the obstacle measured. In the $x - y$ plane (Fig. 8- (a)), the shape including the traffic signs and the contours of the ceiling lamp in the tunnel is better captured by comparing to the actual picture. In the depth direction $z - y$ plane (Fig.8- (b)), the position of traffic plate and the lamp could be estimated from the

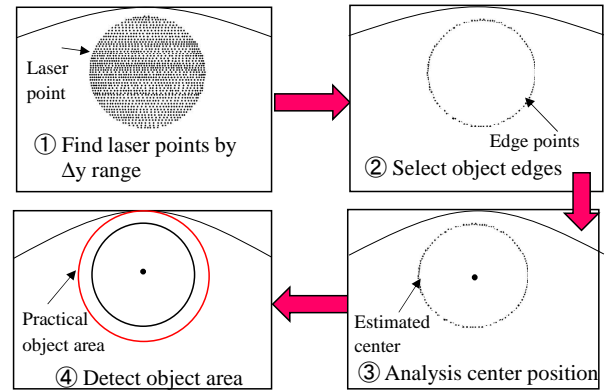


Fig.5 Analysis flow for estimating the position and shape of the obstacle by 3-D Laser Range Finder

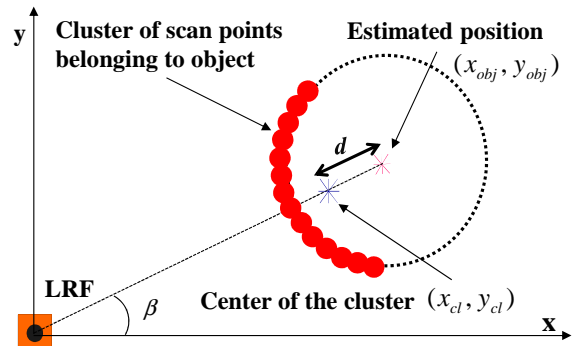


Fig.6 Estimation for center position of circle using the CDM method

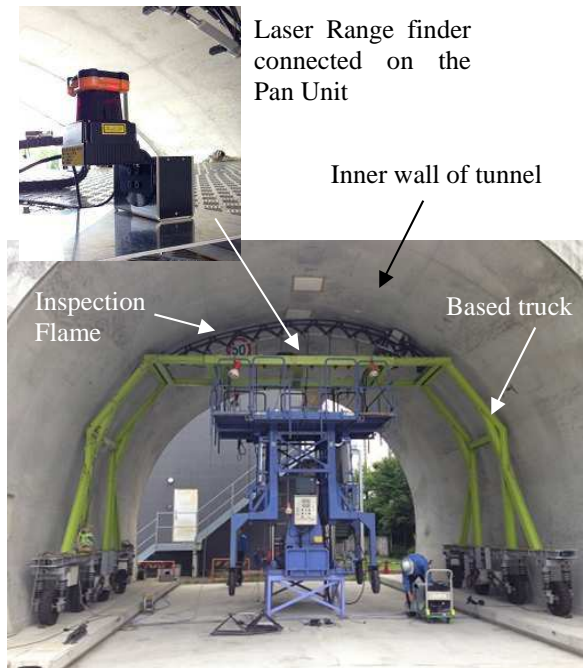


Fig.7 Real simulated tunnel constructed for the experiment and view of based truck

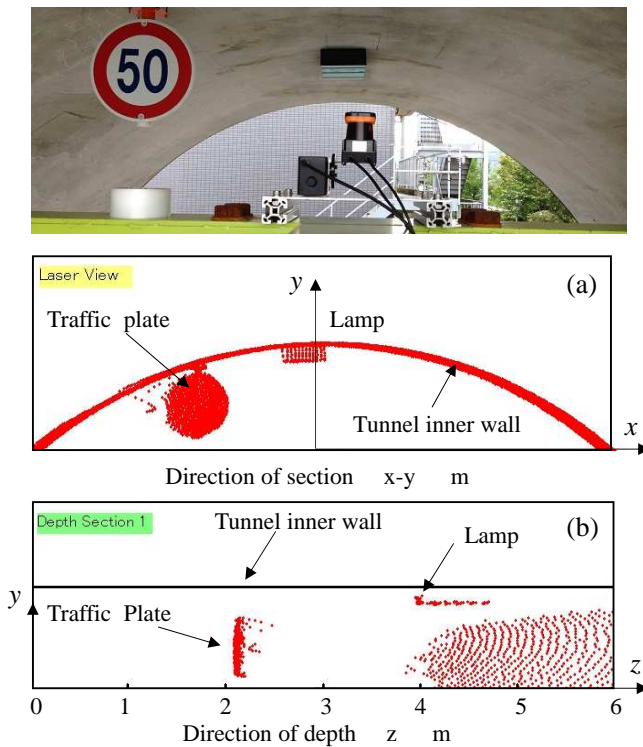


Fig. 8 Obstacles state and positions measured by LRF

portion where the reflection points of the laser are densely concentrated, and it was confirmed that the position was also nearly accurate .

Based on the obstacle data in the $x - y$ plane, its center position was calculated using the analysis flow in Fig.5. As shown in Fig.9 - (a), (b), the center position of each obstacle was obtained from the contour position of the aggregate data, and it was confirmed that the position coincided with the actual position with error accuracy of 10 mm or less. Measurement and analysis, processing time of data was about 1 minute, and it will be possible to detect obstacles sufficiently within the time of inspection work using the guide frame.

3 Shape Control of Variable Guide Frame

In chapter 3, we explain the development of an inspection mobile truck which can avoid obstacles (discharge duct device, lighting lamp, display board, etc.) by using a variable shape frame adaptable to the tunnel shape. In order to create a complicated frame shape avoiding any obstacle on the ceiling surface of the tunnel, we simulated the shape of the guide frame by mathematical method and simulated the frame shape.

3.1 Structure of Variable Guide Frame

The proposed guide frame was constructed on several VGT elements. This VGT (Variable Geometry Truss)

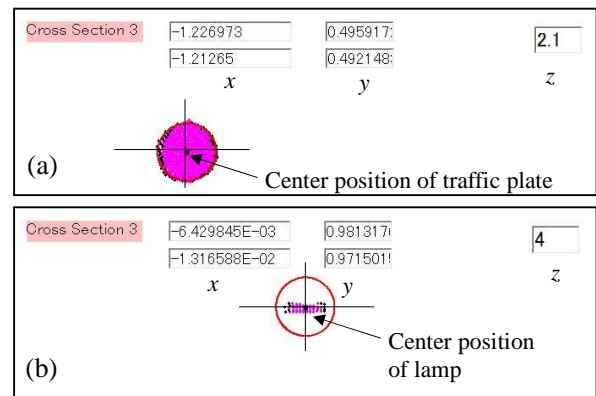


Fig. 9 Estimation of the center position of each obstacle

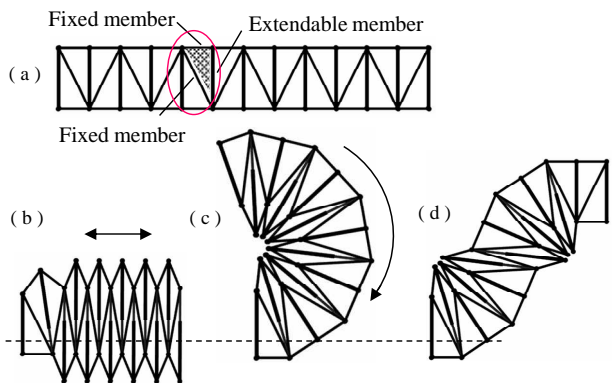


Fig. 10 Example of shape change of VGT structures

was very simple truss structure composed of extendable members, fixed members and hinges, as showing in Fig. 2. By controlling the lengths of the extendable members, it was possible to create various truss shapes. When extendable members are extended simultaneously, the VGT structure was changed like a spring stretching from (a) to (b). When the extendable members are extended alternately, the structure was changed to a circular shape (c) Moreover, when they are extended optionally and their length were controlled, the structure could be changed into any intended shape (d).

In this case, the basic shape of guide frame was an arch structure and its two edges were supported on the protection frame. Though the guide frame was changed flexibly by VGTs shape, the shape was limited by upper side of tunnel wall and traffic space area. So, to avoid projecting obstacle in the tunnel space, it was necessary to correspond to the shape of the guide frame close to the section shape of the obstacle as much as possible. Knowing the obstacle location and shape from the drawing map before inspection, the shape of obstacles as speed plate, blower and side lights were able to simulate by motion analysis. In an actual inspection, the shapes of obstacle were detected by the data of laser range finder continually [6], [7].

3.2 Frame Analysis by Inverse Kinematics

3.2.1 Basic Equation and Shape of Frame

As analysing the arch structure composed of VGT, the whole of guide frame was assumed to be a cantilever structure as indicated in Fig.10-(a). The frame can replace a robot manipulator combining two fixed-length members in series. When the supported edge of frame was $q(x_0, y_0)$, the top $q(x, y)$ of the x, y co-ordinates of the frame combined with n ($n \geq 2$) VGT sets was given by Eq. (7) and Eq.(7) using each hinge angle θ_j . ($j=1, 2, 3, \dots, n$),

$$q(x, n) = l_0 \cdot \sum_{k=1}^n \cos \left\{ \sum_{j=1}^k \theta_j \right\} \quad (7)$$

$$q(y, n) = l_0 \cdot \sum_{k=1}^n \sin \left\{ \sum_{j=1}^k \theta_j \right\} \quad (8)$$

Where, l_0 was the length of diagonal member of the frame. To transform the shape of arch frame, some hinge positions on the frame only had to change in proportion to target shape. However, for an intended frame shape fixed by equations (1) and (2), it was quite difficult to solve these equations analytically and to decide the angle because the frame was a very highly redundant. In this case, inverse kinematics analysis was applied.

Considering a temporal change of the whole of the frame, the top edge modifying the original point by inverse analysis to all VGT angle velocity $\dot{\theta}_j$, a shape change of frame was absorbed according to the arch.

$$\dot{\theta}_i = J^{-1} \cdot \dot{q}_i(x, y) \quad (9)$$

Where, J^{-1} indicates inverse Jacobean Matrix ($2 \times n$). However J^{-1} isn't necessarily decided because J is not a regular system in $n > 2$. In this case, the suitable matrix such a pseudoinverse matrix $J^\#$ was generally induced instead of J^{-1} . Iterating such modification of shape changes, the shape of original arch was able to carve partially to extent in which the obstacle could be evaded.

3.2.2 Shape Change of Guide Frame Avoiding Obstacles

Applying an inverse analysis in the previous chapter 3.2.1, the shape of the frame that avoided the obstacle was analyzed. First of all, a virtual obstacle was positioned on the perpendicular line of the obstacle. The position of a virtual obstacle was gradually lowered, and the frame shape was changed so that surroundings of the obstacle should not come in contact with the frame.

Fig.11-(a)~(d) show the shape change of the arch frame by simulation results. Moving the vertical obstacle, the arch frame was indicated to change like avoiding the obstacle. Finally, a virtual obstacle came in succession at the position of a real obstacle, and the

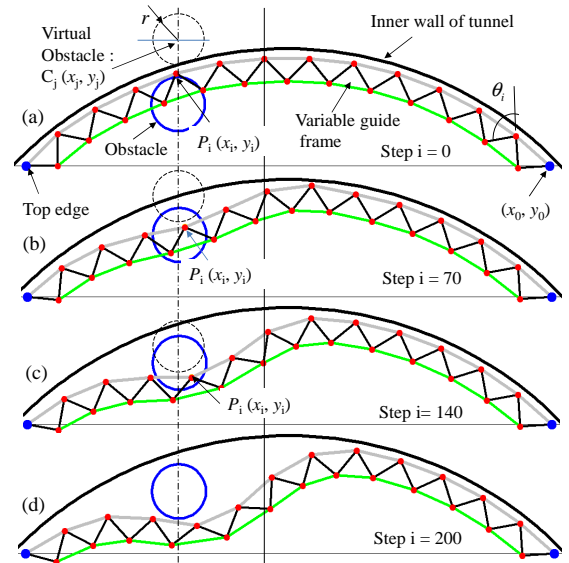


Fig. 11 Shape simulation of VGF to avoid obstacle



Fig. 12 Shape control of guide frame in model tunnel

shape of a final arch frame was decided. As for the shape of the arch frame, it was understood that it was very smooth, no useless movement and two support positions were also the same.

Fig.12 shows the result of experiment in actual model tunnel using variable guide frame. With the real arch frame of 6 m in length, similar shape was able to be also achieved by referring to the simulation result very short times.

3.3 Frame Analysis by Spline Function

3.3.1 Shape Determination Flow of Guide Frame

Fig. 13 shows the flow for determining the shape of the guide frame according to the position and size of the obstacle in the tunnel.

- ① Position and shape recognition of obstacles by LRF
- ② Select multiple points to avoid obstacles on tablet screen
- ③ Determining the shape of the guide frame by spline interpolation function
- ④ Select the element frame according to the determined shape, perform the shape simulation, adjust the defect in the shape change process
- ⑤ Transfer the contents of ④ to the actual frame control device and change the shape of the guide frame

In this flow, it is possible to continuously perform the shape analysis and determination, the transition from the obstacle measurement to the actual system. However, in actual work, guide frames are always in operation by tunnel inspection, and obstacles must be safely avoided in the meantime. In the following, we will discuss ways to enable shape analysis from ② to ③.

3.3.2 Shape Analysis of Guide Frame

To the initial guide frame shape, the overall shapes for avoiding obstacles were mathematically combined by the spline interpolation function.

Spline interpolation is a method of combining arbitrary shapes with polynomials to form a continuous shape. Assuming a function that interpolates the section (x_j, x_{j+1}) , the piecewise polynomial $S_j(x)$ is expressed by the Equation (10).

$$S_j(x) = a_j(x - x_j)^3 + b_j(x - x_j)^2 + c_j(x - x_j) + d_j \quad (j = 0, 1, 2, \dots) \quad (10)$$

In order for this cubic equation to be a smooth curve, it is assumed that the value of the first derivative and the second derivative of $S_j(x)$ are equal, and the value of the second derivative at the start point x_0 and the end point x_n is 0. By applying the above conditions to each equation for several interpolation points, the coefficient of function a_j, b_j, c_j, d_j was calculated, and the function by the spline interpolation was determined.

Here, each coefficient was determined as follows;

$$a_j = \frac{S_j''(x_{j+1}) - S_j''(x_j)}{6(x_{j+1} - x_j)} \quad (11) \quad b_j = S_j''(x_j) / 2 \quad (12)$$

$$c_j = \frac{y_{j+1} - y_j}{(x_{j+1} - x_j)} - \frac{(x_{j+1} - x_j)(2S_j''(x_j) + S_j''(x_{j+1}))}{6} \quad (13)$$

$$d_j = y_j \quad (14)$$

3.3.3 Estimation of Guide Frame Shape avoiding obstacles

Using the method in the previous section, several interpolation points (x_j, y_j) were determined so as to avoid obstacles, and the constants of the piecewise function were calculated using equation (10). However, if the spline function $S_j(x)$ obtained for the selected piecewise interpolation points do not satisfy the condition of $S_j(x_j) < C(x_j)$ for avoiding obstacles for all of the functions, the calculation is repeated by using $(y_j - \Delta y)$ reduced from Δy to y_j for x_j , and the each coefficient of $S_j(x)$ is calculated repetitively until the designed conditions were satisfied. Here, $C(x_j)$ is shown the shape function of the obstacle.

(1) Example of obstacle (a)

The shape of a circular obstacle suspended from the left side of the tunnel ceiling was analyzed using spline

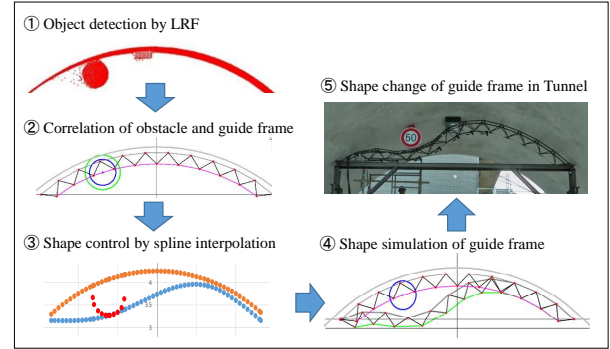
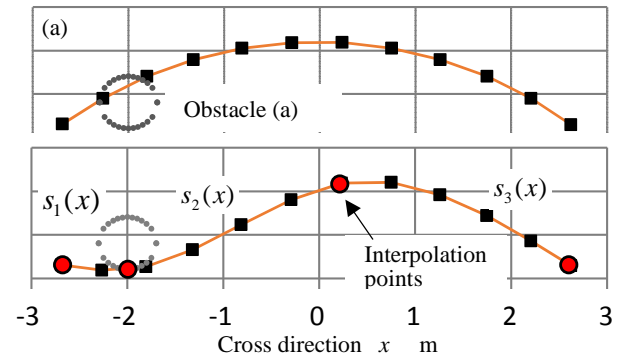


Fig. 13 Shape decision flow of guide frame to avoid objects

Table 2 Each constant value of spline function

$S_j(x)$	a_j	b_j	c_j	d_j
1	0.1966	0	-0.1738	3.156
2	-0.1167	0.4108	0.1081	3.101
3	0.05179	-0.3712	0.1965	4.092



(a) Shape decision of spline function for obstacle (a)



(b) Shape control of guide frame for traffic plate

Fig. 14 Shape decision of guide frame to avoid obstacle

interpolation function. Table 2 shows the values of the respective coefficients for the equation (10) where the number of interpolation points is 2. The result of changing the shape of the guide frame using this coefficient is shown in Fig. 14- (a). It can be seen that the shape of the guide frame analyzed by spline interpolation with respect to the initial shape is a shape smoothly obstructing obstacles. A similar shape change (Fig. 14- (b)) is obtained in experiments on similar obstacle positions.

(2) Example of obstacle (b) and (c)

A shape that avoids an obstacle when the obstacle is in the center was estimated by the same method as (1) above. In the example of (b) as discharge fun, the interpolation point is placed at the bottom of a circular obstacle, in the example of (c) as lighting lamp, the interpolation point is placed at the lower end of a rectangular obstacle, and the uneven shapes that avoid obstacles by combining the five functions were created as indicated in Fig. 15.

From the above results, by using this method, it is possible to determine the shape of the guide frame for avoiding any obstacle.

4 Conclusion

In this research, we introduced a technology that can inspect the tunnel ceiling surface without regulating the tunnel traffic by applying the variable shape frame for inspection that can conform to the tunnel shape.

First of all, the tunnel ceiling area which is an obstacle of the guide frame was searched using LRF. By combining a planar laser sensor and a pan unit, the stereo measurement system was constructed. From the results of measurement and analysis by LRF, it was found that the position of the obstacle almost agrees with the actual value, and it was expected that it could be applied sufficiently to the actual measurement.

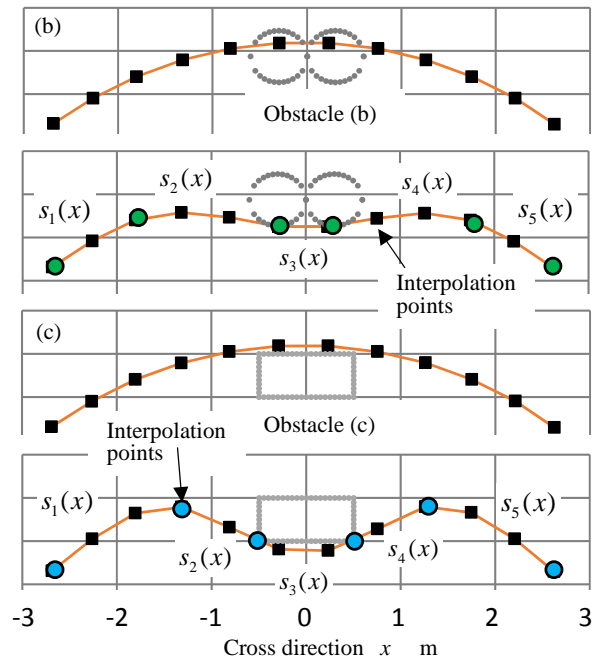
Next, we propose a method to analyzed the shape of the guide frame by inverse analysis and spline interpolation in order to create complicated frame shape avoiding arbitrary obstacles on the tunnel ceiling surface. When using the inversed analysis, the shape change was created smoothly, however, since each frame undergoes a subordinate change, it is not very effective for complicated shapes. On the other hand, in the case of using spline interpolation, since the function classification can be divided according to the shape of the obstacle, complicated obstacles can be dealt with.

In the future, we will establish a control method to continuously change the shape of the guide frame from the obstacle search in the toll, and to apply it to the actual inspection system.

Finally, the author thanks all who supported the development of the movable arch structure and its accompanying external panel. Further, a part of this research is executed by the contract research from NEDO (New Energy and Industrial Technology Development Organization) for SIP.

References

[1] F. Inoue, T. Uchiyama, S. Nakamura and Y. Yanagihara, "Development of Variable Guide Frame to Inspect Inner Wall Tunnel (Part 1;



(a) Shape decision of spline function for obstacle (b), (c)



(b) Shape control of guide frame for traffic sign

Fig. 15 Shape decision of frame to avoid obstacle (b), (c)

Structure of Guide Frame and Shape Analysis)", Proceedings of the 6th International Conference on Advanced Mechatronics (ICAM2015), Tokyo, Japan, PP. 284-285,2010..

- [2] H. Fujii, A. Yamashita and H. Asama, "Defect Detection with Estimation of Material Condition Using Ensemble Learning for Hammering Test", Proceedings of the 2016 IEEE International Conference on Robotics and Automation, pp.847-3854, Stockholm (Sweden), 2016.
- [3] H. Tamura, T. Sasaki, H. Hashimoto and F. Inoue, "Circle Fitting Based Position Measurement System Using Laser Range Finder in Construction Fields," 2010 IEEE/RSJ Intl. Conf. on Intelligent Robots and Systems, pp.209-214, 2010.
- [4] N. Chernov and C. Lesort, "Least Square Fitting of Circles", *Journal of Mathematical Imaging and Vision*, Vol. 23, pp. 239-251, 2005..
- [5] Fumihiko Inoue, Takeshi Sasaki, Xiangqi Huang and Hideki Hashimoto, "A Study on Position Measurement System Using Laser Range Finder

- and Its Application for Construction Work ” ,
Journal of Robotics and Mechatronics, Vol. 26,
No.1, pp. 226-234, 2012.
- [6] Fumihiko Inoue, “A Study on Adaptive Structure
Applying Variable Geometry Truss (Mechanism of
Movable Arch Roof with External Panel)”Journal
of Robotics and Mechatronics, Vol. 21, No.2,
pp.172-178, 2009.
- [7] Fumihiko Inoue, “A Study on Optimum Shapes
and Motion of Movable Arch Structure By
Variable Geometry Truss”, Proceeding of The 9th
Asian Pacific Conference on Shell and Spatial
Structures (APCS2009) , Nagoya, Japan, pp.121-
128, 2009.5